6 Tsunami Early Warning System: An Indian Ocean Perspective

Prasad K. Bhaskaran* **and P.C. Pandey**

1. INTRODUCTION

Tsunamis are considered the most devastating natural hazard on coastal environments ever known. Densely populated cities on coastal belts are the engines of economic growth and the centers of innovation for global economy and hinterlands of respective nations. As we know most of global cities are located near the coast facilitating trade and commerce. They are also located near the mouths of major perennial rivers which serve as conduits for commerce connecting rest of the world. These locations place major cities at a greater risk of natural hazards viz., cyclones, flooding, sea-level rise, tsunamis, etc. With the increasing intensity of economic exploitation in coastal belts, there is also an increase in socio-economic consequences resulting from the hazardous action of tsunami waves generated from submarine seismic activity and other causes. On 26 December 2004, the countries within the vicinity of East Indian Ocean experienced and witnessed the most devastating tsunami in recorded history. This tsunami was triggered by an earthquake of magnitude 9.0 on the Richter scale at 3.4° N, 95.7° E off the coast of Sumatra in the Indonesian Archipelago at 06:29 hrs IST (00:59 hrs GMT).

Historical records of past tsunamis reveal that the most damaging world tsunamis generated by earthquakes during the past five decades are: (i) 1952 – Kamchatka Peninsula (Russian Far East): 18–19 m high (more than 2000 fatalities); (ii) 1960 – Chile: 25 m high (more than 500 fatalities); (iii) 1964 – Alaska: 67 m (more than 100 fatalities reported); and (iv) 26 December 2004 - Indian Ocean: up to 30 m high (more than 200,000 people dead) and 12 countries affected in three continents. The run-up levels associated with the past Indian Ocean tsunamis are summarized in Table 1.

While earthquakes could not be predicted in advance, once the signatures of an earthquake is detected it would have been possible to give warning of a potential Tsunami to the coastal stations. Such a warning system at present is in place across the Pacific Ocean. However, the tsunami warning system in the Indian Ocean had been set up quite recently after the 2004 event. In addition, coastal dwellers within the Pacific Ocean littoral belt are educated to get high ground quickly following waves. However, those in the Indian Ocean are quite unaware. In less than a day, tsunamis can travel from one side of the ocean to the other. People living near areas where large earthquakes occur may find that the tsunami waves will reach their shores within minutes of the earthquake. For these reasons, the tsunami threat for many areas, e.g., Indonesia, Philippines, Java, etc. can be immediate for tsunamis resulting from nearby earthquakes which take only few minutes to reach coastal areas, in comparison with sufficient response time for tsunamis from distant earthquakes which take approximately about 3 to 22 hours reaching other coastal destinations.

Tsunamis are rare in the Indian Ocean as the seismic activity is much less than what exist in the Pacific. Historical records state that there have been seven tsunamis set off by earthquakes near Indonesia, Pakistan and one at Bay of Bengal. Earthquakes occur due to collision of plates at their boundaries.

*Corresponding Author

Table 1. Summary of tsunami occurrences in the Indian Ocean during 1700-2007 period

Sl. No.	*Affected location*	*Run-up height (m)*	*Date/Year*	*Earthquake magnitude at source*	*Source location*
1	Tributaries of Ganges River (Bangladesh)	1.83	12 April, 1762	N.A.	Bay of Bengal
2	Port Blair, Andaman Islands	4.00	19 August, 1868	MW 7.5	Bay of Bengal
3	Car Nicobar Islands, Nicobar Islands	0.76	31 December, 1881	MS 7.9	Car Nicobar Islands, Andaman Sea
4	Dublat, India	0.30			
5	Nagapattinam, India	1.22			
6	Port Blair, Andaman Islands	1.22			
7	Chennai	1.5 (wave height)	26 August, 1883	Krakatao Volcanic Eruption	Islands of Java and Sumatra
8	Andaman & Nicobar Islands	N.A.	26 June, 1941	MW 7.7	Andaman Sea (12.5°N; 92.57°E)
9	Mumbai, India	1.98	27 November, 1945	MS 8.3	Arabian Sea (24.5°N; 63°E)
10	Karachi, Pakistan	1.37			
11	Ormara, Pakistan	13.0			
12	Pasni, Pakistan	13.0			
13	Victoria, Mahe Islands, Seychelles	0.30			
14	Not felt in India	-	19 August, 1977	MS 8.1	West of Sumba Islands, Indonesia
15	Cocos Islands, Australia	0.30	18 June, 2000	MS 7.8	Arabian Sea
16	13 countries surrounding Indian Ocean rim directly affected	34.90	26 December, 2004	MS 9.0	West coast of Northern Sumatra, Indonesian Archipelago
17	Indonesia	1.0	28 March, 2005	MS 8.6	Indonesia
18	Java	2.0	17 June, 2006	MS 7.7	Indonesia

Source: Information from the website of NGDC (National Geophysical Data Centre, NOAA, USA; http://www.ngdc.noaa.gov/hazard/tsu.shtml).

Scientists now believe that one plate that comprised the landmass from India to Australia has broken up into two (Orman et al., 1995). The earthquake location of recent 2004 Indian Ocean tsunami was near the meeting point of Australian, Indian and the Burmese plates. Scientists have advocated that this is a region of compression as the Australian plate is rotating counterclockwise into the Indian plate. The implication of this also means that a region of seismic activity has become active in the South-eastern Indian Ocean which has potential of triggering another deadly tsunami. Within the close vicinity of India, there are two potential tsunamigenic zones: Andaman-Sumatra trench (East India) and the Makran coast (West India).

Tsunamis are known as long gravity waves, and hence their travel time in the ocean depends only on the water depth and gravity, at least to the zeroth-order. As of today, no technology exists to predict a tsunami event well in advance (Synolakis, 1995). Contrary to popular belief, the tsunami travel times do

not depend upon the magnitude of the under-water disturbance that generated the tsunami. For the Pacific Ocean, it has been clearly demonstrated that the computed tsunami travel times using the zero-order approximation are correct to plus or minus one minute for each hour of travel. The advantage of this zero-order approximation is that tsunami travel times to selected locations around the rim of the Indian Ocean as well as to selected island sites can all be pre-computed in advance once and for all. This set of information can be stored in the electronic format as well as a tsunami travel time atlas format and can be quickly accessed in real tsunami events with a minimum effort.

Isochrome charts on tsunami travel time were first made in 1947 by the American Coastal Service after the Aleutian disastrous tsunami in the Pacific coast (Zetler, 1947). Subsequently, in 1971 these charts were evaluated and about fifty such charts were used by the tsunami warning system (Holloway et al., 1986). In concurrence with the disastrous tsunami of Hawaii on 1 April 1946 (Okal et al., 2002) from an earthquake in the Aleutian Islands of USA, a Pacific Ocean tsunami warning system was established based in Ewa Beach, Oahu Island, Hawaii, USA. In the immediate vicinity of islands, the catastrophe resulting from a tsunami is advocated as enormous (Yeh et al., 1994).

The goal of this chapter is to present a brief review on tsunamis which affected Indian sub-continent, current status of tsunami warning system for the Indian Ocean, and methodology used in the construction of tsunami travel time charts for the Indian Ocean. Further, the importance of artificial neural network (ANN) to expedite warnings has been demonstrated, which is considered an essential pre-requisite for an early warning system in the Indian Ocean.

2. REVIEW ON TSUNAMIS AFFECTING THE INDIAN SUBCONTINENT

Though majority of reported tsunamis are from countries surrounding the Pacific Ocean rim, there are also few reported cases of tsunamis in the Indian Ocean. Considering the vast length of Indian coastline (7516 km), the threat arising from tsunami-genic event is potentially hazardous. From our past experiences, the tsunami-genic earthquakes occurred mostly at these three locations, viz.; (i) the Andaman Sea, (ii) geographical area about 400-500 kilometers South south-west off Sri Lanka, and (iii) in Arabian Sea about 70-100 km south off Pakistan coast. The oldest record of tsunami in the Indian Ocean dates back to November 326 B.C. earthquake near the Indus Delta (presently the Kutch region) where a major earthquake destroyed the Macedonian fleet (Lietzin, 1974). Historical records of tsunamis in the Indian Ocean reported 1.5 m at Chennai resulting from August 8, 1883 Krakatao volcanic eruption in Indonesia. Also, an earthquake of magnitude 8.25 occurred about 70 km south of Karachi, Pakistan on November 27, 1945. This resulted in a large tsunami magnitude of about 11.0 to 11.5 m high in the west coast of India (Kutch region) (Pendse, 1945). There are few more cases of earthquakes with a magnitude less than 8.0 which have given rise to some smaller tsunamis. Bapat et al. (1983) reported a few more earthquakes along the coast of Myanmar.

In the Andaman Sea, an earthquake of magnitude 8.1 occurred on June 26, 1941 resulting in a tsunami affecting the east coast of India. According to non-scientific sources, the heights of tsunami waves were in the order of 0.75 to 1.25 meters as no tide-gauges were in operation then. This was the strongest earthquake ever recorded in the Andaman & Nicobar Islands prior to which was the 1881 Nicobar Islands earthquake (magnitude 7.9 on the Richter scale). Hindcast studies employing mathematical calculations suggested that the height could be in the order of 1.0 meter. It is believed that nearly 5,000 people were killed by this tsunami in the east coast of India. Local newspaper sources are believed to have mistaken the deaths and damage to a storm surge; however, a search of meteorological records (Murty, 1984) does not show any storm surge on that day in the Coromandel Coast. Tremors from this earthquake were felt in cities along the Coromandel (eastern) Coast of India and even in Colombo,

Sri Lanka. This earthquake was followed by several powerful aftershocks (Tandon et al., 1974). Two events of magnitude 6.0 struck within 24 hours of the main shock on June 27, 1941. The first occurred at 07:32:47 UTC and was followed by another at 08:32:19 UTC. Consequently, these were then followed by 14 earthquakes of magnitude 6.0 until January 1942.

Considering the build-up of seismic activity in the Southeastern Indian Ocean and associated calamities which resulted from the past tsunami-genic events, a comprehensive tsunami travel time (TTT) atlas for the Indian Ocean was developed by Prasad et al. (2005) which can serve as an important tool for the early warning of tsunami. We discuss in subsequent sections how this information from the TTT atlas can be used in the context of ANN to reduce response time for an early warning system in the Indian Ocean.

3. CURRENT STATUS OF TSUNAMI WARNING SYSTEM FOR THE INDIAN OCEAN

Recognizing the imperative to put in place an Early Warning System for the mitigation of oceanogenic disasters that cause severe threat to nearly 400 million population living in the coastal belt with devastation of life and property, and further driven by the national calamity due to the Indian Ocean Tsunami of December 26, 2004, the Ministry of Earth Sciences (MoES), Government of India, has taken up the responsibility of establishing a National Tsunami Early Warning System (NTEWS). The Warning System has been established by MoES as the nodal ministry at a cost of Rs. 1,250 million in collaboration with the Department of Science and Technology (DST), Department of Space (DOS) and the Council of Scientific and Industrial Research (CSIR), Government of India. The National Tsunami Early Warning Centre has been set up at the Indian National Centre for Ocean Information Services (INCOIS), Hyderabad, Andhra Pradesh, India.

Tsunami-genic zones that threaten the Indian coast have been identified by considering the historical tsunamis, earthquakes, their magnitudes, location of the area relative to a fault, and also by tsunami modeling. The east and west coasts of India including the island regions are likely to be affected by tsunamis generated mainly by subduction zone related earthquakes from the two potential source regions, viz., the Andaman-Nicobar-Sumatra island arc and the Makran subduction zone north of Arabian Sea. The Indian Tsunami Early Warning System comprises a real-time network of seismic stations, Bottom Pressure Recorders (BPR) and tide gauges to detect tsunami-genic earthquakes and to monitor tsunamis.

The Early Warning Centre receives real-time seismic data from the national seismic network of the India Meteorological Department (IMD), New Delhi, and other international seismic networks. The system detects all the earthquake events of magnitude greater than 6 occurring in the Indian Ocean in less than 20 minutes of occurrence. BPRs installed in the deep ocean are the key sensors to confirm the triggering of a tsunami. The National Institute of Ocean Technology (NIOT) has installed four BPRs in the Bay of Bengal and two BPRs in the Arabian Sea. In addition, NIOT and Survey of India (SOI) have installed 30 Tide Gauges to monitor the progress of tsunami waves. Integrated Coastal and Marine Area Management (ICMAM) has customized the tsunami model for five historical earthquakes and the predicted inundation areas. The inundated areas are being overlaid on cadastral level maps of 1:5000 representative scales. These community-level inundation maps are extremely useful for assessing the population and infrastructure at risk. High-resolution coastal topography data required for modeling is generated by the National Remote Sensing Agency (NRSA), Government of India, using ALTM and CARTOSAT data. INCOIS has also generated a large database of model scenarios for different earthquakes that are being used for operational tsunami early warning.

Communication of real-time data from seismic stations, tide gauges and BPRs to the early warning centre is very critical for generating timely tsunami warnings. A host of communication methods are employed for timely reception of data from the sensors as well as for dissemination of alerts. Indian Space Research Organization (ISRO), Bangalore, has made an end-to-end communication plan using INSAT. A high level of efficiency is being built into the communication system to avoid single point failures.

A state-of-the-art early warning center is established at INCOIS (Indian National Centre for Ocean Information Services) located in Hyderabad, Andhra Pradesh, with all the necessary computational and communication infrastructure that enables reception of real-time data from all the sensors, analysis of the data, generation and dissemination of tsunami advisories following a standard operating procedure. Seismic and sea-level data are continuously monitored in the Early Warning Centre using a custom-built software application that generates alarms/alerts in the warning centre whenever a pre-set threshold is crossed. Tsunami warnings/watches are then generated based on pre-set decision support rules and disseminated to the concerned authorities for action, following a Standard Operating Procedure. The efficiency of the end-to-end system was proved during the large under-sea earthquake of 8.4 M that occurred on September 12, 2007 in the Indian Ocean.

The National Early Warning Centre will generate and disseminate timely advisories to the Control Room of the Ministry of Home Affairs (MHA) for further dissemination to the public. For the dissemination of alerts to MHA, a satellite-based virtual private network for disaster management support (VPN DMS) has been established. This network enables early warning center to disseminate warnings to the MHA, as well as to the State Emergency Operations Centers. In addition, alert messages will also be sent by Phone, Fax, SMS and e-mails to authorized officials. In case of confirmed warnings, the National Early Warning Centre is being equipped with necessary facilities to disseminate the advisories directly to the administrators, media and public through SMS, e-mail, fax, etc. The cyclone warning network of IMD and electronic ocean information boards of INCOIS could be effectively used for disseminating warnings directly to the public.

Periodic workshops will be organized in future for the user community by INCOIS to familiarize them with the use of tsunami and storm surge advisories as well as inundation maps. Easily understandable publicity material on earthquake, tsunami and storm surges will be generated by INCOIS and will be distributed in future to the general public for awareness.

4. ORGANIZATION OF TRAVEL TIME CHARTS

The locations for the present study have been chosen mainly for population centers around the Indian Ocean (Fig. 1). Also, any location deserving special consideration, even if it is not a major population center, has also been included. Database on countries surrounding the Indian Ocean rim was first identified. Accordingly, 35 countries surrounding the Indian Ocean has been selected listing major cities and population. Table 2 summarizes the country name and number of locations used in this study.

The study domain encompasses starting at the south-eastern end of the Indian Ocean (west coast of Australia) and proceeding northward to Bay of Bengal, then to the Arabian Sea. It should be noted that the Red Sea and the Persian Gulf (Arabian Gulf) are part of the Arabian Sea system which have experienced Tsunamis in the past, one notable example being the Arabian Sea tsunami of November 27, 1945. From the Red Sea, we proceed southward along the east coast of Africa until the Cape of Good Hope, and that limits the geographic domain for the TTT computation, as our interest here is only the Indian Ocean and not the Atlantic Ocean. Figure 2 depicts the earthquake locations for which TTT computations were conducted.

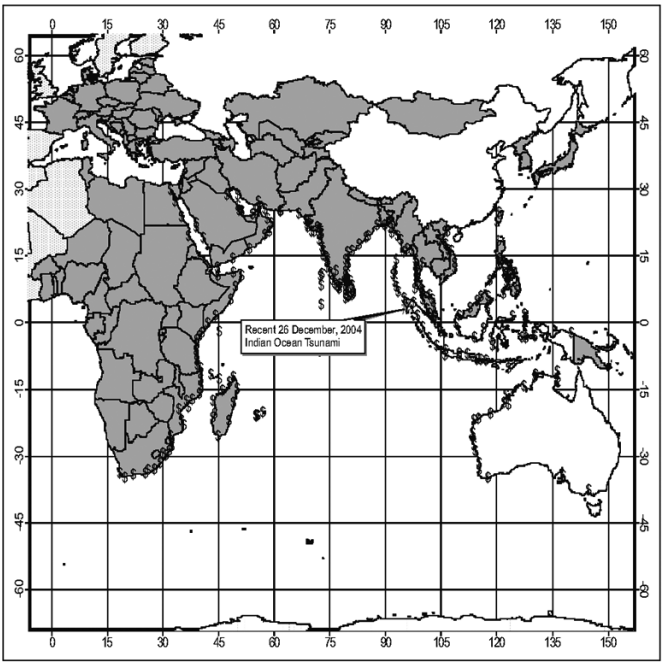

Fig. 1 Geographical locations of 35 countries in the Indian Ocean rim, for which the travel time of tsunami waves had been numerically computed by Tsunami Travel Time (TTT) model using the epicenter location (95.947°E; 3.307°N) of the recent (26 December, 2004) energetic event in the Indian Ocean.

Table 2. List of countries and corresponding number of coastal stations used for generating Tsunami Travel Time (TTT)

Country	*Number of locations*	*Country*	*Number of locations*	*Country*	*Number of locations*
Australia	19	Malaysia	12	Singapore	1
Bahrain	1	Maldives	1	Somalia	8
Bangladesh	3	Mauritius	1	South Africa	11
Brunei	1	Mozambique	9	Sri Lanka	15
Comoros	2	Myanmar	9	Sudan	2
Egypt	3	Oman	5	Taiwan	2
India	47	Pakistan	3	Tanzania	7
Indonesia	31	Philippines	11	Thailand	6
Iran	3	Qatar	2	U.A.E.	3
Kenya	3	Reunion	4	Vietnam	8
Kuwait	1	Saudi Arabia	3	Yemen	2
Madagascar	10	Seychelles	1		

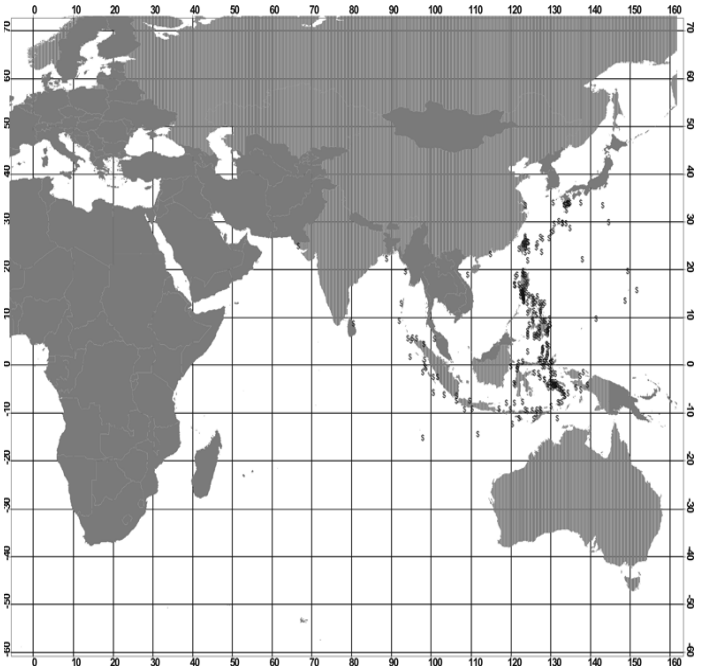

Fig. 2 Geographical coordinates of 250 past earthquake events in the Indian Ocean for which TTT were computed.

5. COMPUTATION AND DESCRIPTION OF TSUNAMI TRAVEL TIME CHARTS

The technique used to compute travel times over the entire grid is an application of Huygens principle which states that all points on a wave-front are point sources for secondary spherical waves. From the starting point, times are computed to all surrounding points. The grid point with minimum time is then taken as the next starting point and times are computed from there to all surrounding points. The starting point is continually moved to the point with minimum total travel time until all grid points have been evaluated. In the countries surrounding the Indian Ocean rim, 250 locations as mentioned above were selected for this study. The travel time of tsunami waves from the epicenter to various coastal regions has been evaluated for all the sample points identified.

On 26 December 2004, the countries in the Eastern Indian Ocean experienced the most devastating tsunami in recorded history (Bindra, 2005). This tsunami was triggered by an earthquake of magnitude 9.0 on the Richter scale off the coast of Sumatra in the Indonesian Archipelago at 06:29 hrs IST (00:59 hrs GMT). The extent of damage resulting from this tsunami has been cited in the post-tsunami field survey (Chapman, 2005). The dispersive signals of this energetic event were recorded by hydrophones and seismic stations in coastal locations around the Indian Ocean rim (Hanson and Bowman, 2005). The computational example for this Indian Ocean tsunami using our computational algorithm is shown in Fig. 3.

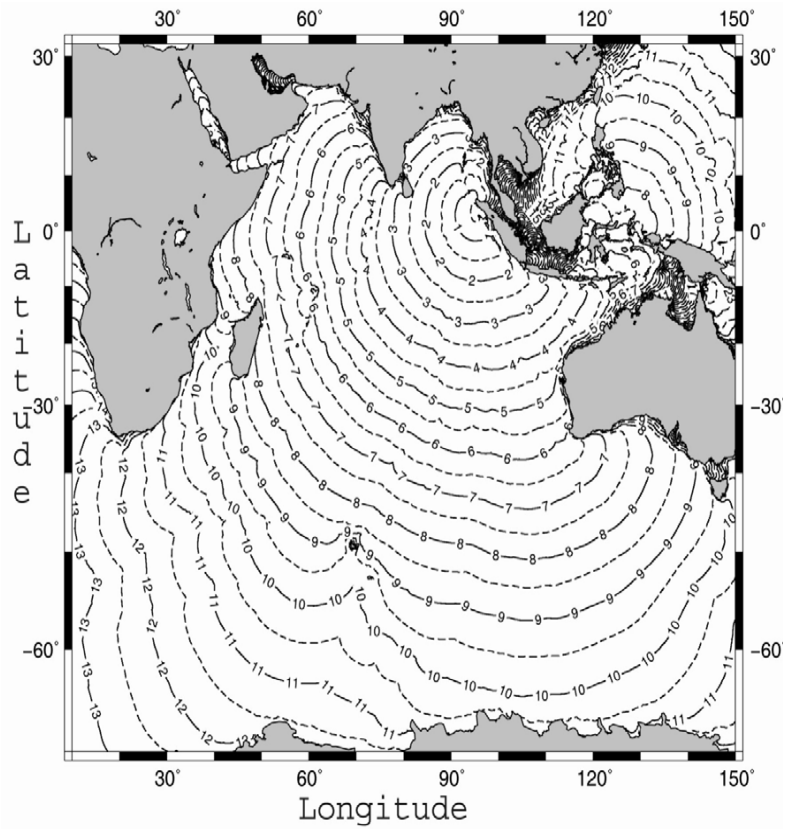

Fig. 3 Travel time of tsunami waves that resulted from the 26 December, 2004 event in the Indian Ocean. The contour intervals are sampled at every half an hour.

The most basic information a tsunami warning center requires is ETA (Expected Time of Arrival) of the first tsunami wave at selected coastal locations from the area of tsunami generation in the ocean. Almost always, the first wave in a tsunami event is not the wave with the greatest amplitude; nevertheless, tsunami travel time charts are generally constructed for the first wave, rather than the wave with the highest amplitude. Advanced knowledge of travel time for the first wave provides some additional valuable time for the evacuation of people, if and when evacuation is needed. In addition, tsunami travel times can be pre-computed, independent of the seismic moment magnitude of the earthquake, only for the first wave. The heights of the subsequent waves are not known until the event actually happens, and hence no pre-determination of the travel time of the highest wave can be made.

To the zeroth order, tsunami travel times are governed by the long gravity wave formula, which defines the speed of travel of the tsunami as equal to the square root of water depth, multiplied by the acceleration due to gravity (Murty et al., 1987). Of course there are higher order correction terms to the

speed of tsunami travel, based upon dispersion characteristics. While these higher order terms are of scientific interest, nevertheless, for practical purposes, one can ignore the contributions from these terms, and use the simple long wave formula.

The calculation algorithm adopted by the authors for computing the isochromes tables is based on the well-known Huygens method and is actually a group of methods which obtain the time required for passing a given space interval with a given speed (Yuri et al., 1995). In this technique all the nodes of the calculated grid are partitioned into three sets, set M_1 containing the nodes with finally calculated tsunami travel times, set M_2 contains the nodes with preliminary estimated values that may later be refined and set M_3 the nodes with arrival time that has not been obtained yet. Each node (U) is associated with the notion of its domain of influence (S_u) which is aggregate of neighboring nodes satisfying criterion of proximity. It is considered that during one step of an algorithm the perturbation can cover the distance from the specified node only to its nearest pattern neighbors.

At the initial time all the nodes in the domain of the initial perturbation are assigned zero value of the arrival time (T_0) corresponding to the time of beginning of the earthquake and included in the set M_2^0. The remaining nodes of the calculation domain are included in M_3^0. Then the nodes of M_2^0 with patterns not influenced by the ones of the set M_3^0 are transferred to the set M_1^1 and excluded from further calculations. The algorithm afterwards acquires the regular character. Hence, at the nth step the exhaustive search of the nodes from the set M_2^n is performed in order of increasing tsunami travel times known at this point of time.

Let the node $A \in M_2^n$ (1)

and $T_A = \min\{T_{A_i}\}$ (where, $A_i \in M_2^n$); then the node for B such that $B \in S_A$ the tentative estimate (A) of arrival time is found from the relation:

$$T = T_A + T_{AB} \tag{2}$$

where $T_{AB} = \dfrac{2L_{AB}}{C_A + C_B}$ which is the time of perturbation propagation from the node 'A' to 'B'.

Here $L_{AB} = R \times \arccos(\sin\varphi_A \times \sin\varphi_B + \cos\varphi_A \times \cos\varphi_B \times \cos\Delta\psi)$ denotes the distance from node 'A' to 'B' through the great circle arc; 'R' stands for the radius of the earth; and $c = \sqrt{gh_i}$ is the local rate of perturbation propagation (h_i denotes the depth of the i-th node and 'g' the acceleration due to gravity).

In case where, $B \in M_3^n$, relation from (Equation 1) first yields the value of 'T' and the node 'B' itself is transferred to M_2^{n+1}, and if $B \in M_2^n$, the value of 'T' is refined from the minimizing relation:

$$T_B = \min\{T_A, T_A + T_{AB}\} \text{ (where } A \in S_B \cap M_2^n) \tag{3}$$

After the values of T, $\forall B : B \in S_A$ are obtained from Equations 1 and 2, the node 'A' is transferred to the set M_1^{n+1}. This procedure is repeated to the next node $A \in M_2^n$ satisfying the condition (Equation 1) and so on until the set M_2^n is exhausted. For the next (n+1) time step, the algorithm is reproduced without any changes and the computation goes on until step 'k' where all calculation node of the water area are included in the set M_1^k.

For the Pacific Ocean, it has been shown that the travel time charts are accurate to plus or minus one minute, for each hour of travel. There is no reason to expect that the travel time charts will be less precise for the Indian Ocean. This level of error is considered acceptable for tsunami warning purposes. Since, at present one cannot predict precisely the location and time of occurrence of a tsunami-genic earthquake; it is not possible to construct tsunami travel time charts for all possible future tsunamis. In any case,

travel time information is required for coastal locations, where disaster mitigation procedures have to be invoked during real tsunami events. However, tsunami travel time charts are reversible, in the sense that the travel times are exactly the same, no matter in which direction the tsunami travels on a given chart, i.e., from an epicenter in the ocean to a coastal site or vice-versa (i.e., from a coastal site to an epicenter in the ocean). Once a reasonable number of tsunami travel time charts are prepared for the Indian Ocean, for selected coastal and island locations, as well as for all historical tsunami events, it is quite probable that for any future tsunami events, the travel time information that is required could be quickly and effortlessly obtained from these charts.

6. APPLICATION OF ARTIFICIAL NEURAL NETWORK IN TSUNAMI TRAVEL TIME PREDICTION

Artificial Neural Networks (ANNs) are inspired by the biological nervous system. Composed of elements operating in parallel, the network function is primarily determined by connections (weights) between elements. A neural network can be trained to perform a particular function by adjusting the values of these weights between elements. Commonly neural networks are adjusted, or trained so that a particular input leads to a specific target output. The network can be trained based on a comparison of the output and the target until the network output matches the target within a specified error level (supervised learning). In this study, different combinations of input were used to train the network. The trained network can be validated with the data that has not been used for training. If the system performs well with the validation data, the system can be deployed real time to perform a specific job.

Neural networks can be trained to solve problems that are difficult for conventional computers. Neural networks have been trained to perform complex functions in diverse fields of application which include nonlinear regression, classification, identification, pattern recognition and control systems (Hinton, 1992; Navone and Ceccatto, 1994; Bishop, 1995; Venkatesan et al., 1997; Silverman and Dracup, 2000; Li et al., 2005). The supervised training methods are commonly used, but other networks can be obtained from unsupervised training techniques which can be used where there are no input/output pairs as such but only input data. This for instance may be used to identify groups of data (Hopfield Networks).

Neural network approach has been also used to solve inverse problems which include a methodology to assess the severity of a tsunami based on real-time water-level data near the source (Yong et al., 2003). This inverse method which uses tsunami signals in water-level data to infer seismic source parameters is extended to predict the tsunami waveforms away from the source. The present study which involves the prediction of *Tsunami Arrival Time* is within the domain of nonlinear regression where MLP is used to tackle the nonlinearity in the data. A brief description of the MLP used to tackle the prediction problem is provided below.

An MLP (Fig. 4) is a feed forward network consisting of three classes of layers: the input layer, the hidden layers (a network can have several hidden layers) and the output layer. The inputs to the network are given at the input layer and the number of input nodes would be equal to the number of input parameters. The input nodes receive the data and pass them onto the hidden layer nodes (neurons). The neuron model and the architecture of a neural network then determine how the input is transformed into an output. This transformation involves computation and can be represented with detailed mathematical algorithms. The perceptron then computes single output from multiple real-valued inputs by forming a linear combination according to its input weights and then possibly putting the output through a nonlinear activation function. This can be expressed mathematically as (Simon, 1998):

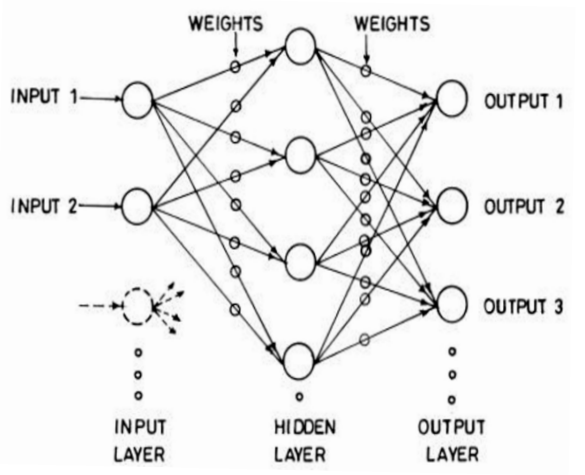

Fig. 4 Structure of an artificial neural network (Bishop, 1995).

$y = \Psi\sum_{i=1}^{N}(w_i x_i + b)$, where w denotes the vector of weights, x the vector of inputs, b the bias and Ψ the activation function. The supervised learning problem of the MLP can be solved with the back-propagation algorithm. This algorithm consists of two steps. In the forward pass, the predicted outputs corresponding to the given inputs are evaluated and in the backward pass, partial derivatives of the cost function with respect to the different parameters are propagated back through the network (Bishop, 1995). It may be noted that chain rule of differentiation gives very similar computational rules for the backward pass as the one in the forward pass. The networked weights can then be adapted using a gradient-based optimization algorithm. The entire computational process is then iterated until the weights have converged (Simon, 1998).

7. DEVELOPMENT OF MODEL FOR TSUNAMI ARRIVAL TIME PREDICTION

The technique used to compute travel times over the study domain is an application of Huygens principle which states that all points on a wave-front are point sources for secondary spherical waves. From the starting point (actual epicenter location), travel times are computed to all surrounding equidistant grid points. The grid point with minimum time is then taken as the next starting point (new location) and computation is performed thereafter to all surrounding points. The starting point is then continually moved to the point with minimum total travel time until all grid points have been evaluated. For the countries surrounding the Indian Ocean rim, 250 coastal locations were selected for this study. The travel time of tsunami waves from the epicenter to various coastal regions were evaluated for all the sample points identified. This technique was used for multiple tsunami-genic locations in the Indian Ocean rim facilitating the development of a comprehensive ETA database (Prasad et al., 2005), which has been used for training the neural network in the present study. For the benefit of the readers, a detailed methodology of ETA computations and further skill assessment with available observations for the 26 December 2004 event in the Indian Ocean was investigated (Prasad et al., 2006).

7.1 Data for Artificial Neural Network

This ANN-based study computes a new travel time chart which is highly efficient in the prediction of ETA to several coastal destinations in the Indian Ocean for any given epicenter location in the study domain. The input to the ANN model comprises the location of the underwater earthquake source viz., latitude and longitude and the ETA from the comprehensive database. In the 250 coastal destinations of countries surrounding the Indian Ocean rim (Fig. 1), ETA for 47 coastal destinations is within the purview of Indian sub-continent. The ANN model for this study has been trained to perform prediction to these 47 coastal destinations. The coastal locations used for this study is chosen mainly from high density population centers depicted in Fig. 2. Minutiae shown in Table 3 list the country name and number of locations taken from the comprehensive database of ETA for the present study. The epicenters of all past tsunamigenic events in the Indian Ocean were compiled from information obtained from NGDC (National Geophysical Data Center, NOAA, Boulder, USA; http://www.ngdc.noaa.gov/hazard/earthqks.html). Figure 2 illustrates the epicenter locations of the past earthquake events (250 locations) having magnitude greater than 6.0 on the Richter scale used in the comprehensive ETA database.

Table 3. Computed Expected Arrival Time (ETA) to 250 coastal stations for the December 26, 2004 tsunami event in the Indian Ocean

Country	*City*	*Population*[#]	*Location*		*Arrival time (hour)*
			Latitude (Degree)	*Longitude (Degree)*	
1. South Africa	Mtunzini	12,050	28.97S	31.77E	11.222
	Durban	2,117,650	29.87S	30.99E	11.002
	Ladysmith	89,087	28.02S	32.66E	10.6756
	Port St Johns	1,46,132	31.62S	29.53E	11.032
	East London	212,323	32.97S	27.87E	11.4353
	Port Elizabeth	1,100,000	33.96S	25.59E	12.131
	Grahamstown	62,640	33.19S	26.31E	12.22
	Mosselbaai	55,100	34.18S	22.13E	12.9163
	Cape Agulhas	26,182	34.83S	20.00E	13.3881
	Pietermaritzburg	229,000	29.36 S	30.23 E	11.1826
	Cape Town	2,350,000	33.93S	18.47E	13.5143
2. Mozambique	Pemba	84,897	12.58S	40.30E	9.34164
	Nacala	158,248	14.31S	40.34E	9.38824
	Angoche	74,624	16.17S	39.97E	9.64704
	Pebane	1,274	17.23S	38.17E	10.2653
	Quelimane	150,116	17.53S	36.58E	11.7402
	Beira	397,368	19.50S	34.52E	13.8161
	Vilanculos	19,371,057	22.02S	35.32E	10.8631
	Inhambane	52,370	23.02S	35.92E	10.3011
	Maputo	966,837	25.58S	32.32E	11.3468
3. Tanzania	Mtwara	1,128,523	10.20S	40.20E	9.07369
	Lindi	791,306	09.56S	39.61E	9.06953
	Kilwa	171,057	08.55S	39.30E	9.31335
	Dar es Salaam	1,292,973	06.50S	39.12E	9.52655
	Tanga	1,642,015	05.05S	39.02E	9.27646

(*Contd.*)

Table 3. (*Contd.*)

Country	*City*	*Population*[#]	*Location*		*Arrival time (hour)*
			Latitude (Degree)	*Longitude (Degree)*	
	Zanzibar	391,002	06.10S	39.20E	9.68088
	Wete	186,013	05.04S	39.43E	9.1367
4. Kenya	Lamu	2,249	02.28S	40.90E	9.14886
	Malindi	64,300	03.12S	40.05E	9.06343
	Mombasa	1,880,000	04.02S	39.43E	9.04207
5. Somalia	Berbera	200,000	10.47N	45.03E	9.17937
	Boosaso	90,100	11.28N	49.18E	8.27345
	Ras Hafun	5,000	10.48N	51.33E	7.79386
	Eyl	682	08.00N	49.82E	7.69955
	Obbia	386	05.33N	48.50E	7.82298
	Mogadishu	1,262,000	02.06S	45.37E	7.8039
	Merca	173,100	01.48N	44.50E	8.18546
	Kisimayo	201,600	00.22S	42.32E	8.51144
6. Sudan	Suakin	10,500	19.08 S	37.17 E	10.3177
	Port Sudan	730,000	19.38 N	37.08 E	13.5179
7. Egypt	Hurghada	182,526	27.15 N	33.50 E	15.492
	Suez	417,610	30.00 N	32.30 E	18.5576
	Al-Ghardaqah	71,800	23.88 N	35.27 E	14.6119
8. Yemen	Aden	519,822	12.45N	45.00E	8.96302
	Al Mukalla	890,246	14.33N	49.02E	8.12144
9. Saudi Arabia	Jeddah	2801481	21.53N	39.17E	14.1548
	Rabigh	31,963	22.50 N	39.05 E	14.0922
	Al Qunfudhah	1,772	19.03N	41.04E	13.8529
10. U.A.E.	Sharjah	320,095	25.20N	55.24E	11.8153
	Abu Dhabi	398,695	24.28N	54.25E	14.8918
	Dubai	669,181	25.271N	55.329E	11.4325
11. Qatar	Doha	285,000	25.15N	51.36E	15.3089
	Dukhan	9,835	25.3N	50.8E	18.6514
12. Bahrain	Manama	143,035	26.236N	50.583E	16.4257
13. Kuwait	Kuwait	28,747	28.59N	47.52E	19.3276
14. Iran	Bandar-e-Bushehr	143,641	28.59N	50.46E	16.2342
	Bandar Abbas	273,578	27.12N	56.15E	10.3892
	Jask	66,128,965	25.642N	57.772E	8.2053
15. Oman	Salalah	156,530	16.56N	53.59E	7.45856
	Sur	66,785	22.34N	59.32E	7.46266
	Muscat	540,000	23.37N	58.36E	7.90009
	Duqm	4,269	19.65N	57.7E	7.60163
	Masirah	841	20.417N	58.833E	7.29651
16. Pakistan	Karachi	9,856,318	24.53N	67.00E	8.43242
	Gwadar	185,498	25.10N	62.18E	7.66909
	Jiwani	25,000	25.117N	61.733E	8.20665
17. Bangladesh	Chittagong	6,545,078	24.05N	91.00E	6.37145
	Cox Bazaar	1,757,321	21.26N	91.59E	4.44494
	Dhulasar	27,046	21.87N	90.23E	5.20506

(*Contd.*)

(*Contd.*)

18. Myanmar	Sittwe	107,620	20.15N	92.09E	3.76803
	Kyaukpyu	19,456	19.45N	93.55E	4.47832
	Sandoway	4,000	18.47N	94.45E	3.94103
	Kadonkani	47,382,633	15.83N	95.18E	5.6117
	Yangon	2,513,023	16.47N	96.10E	4.37541
	Mawlamyine (Moulmein)	219,961	16.30N	97.37E	4.53773
	Tavoy	139,900	14.12N	98.30E	6.14122
	Mergui	177,961	12.43N	98.56E	4.62463
	Kawthaung	41,994,678	10.02N	98.53E	3.87474
19. Thailand	Bangkok	7,506,700	13.45N	100.35E	26.6819
	Surat Thani	153,500	09.06N	99.20E	24.5288
	Songkhla	294,200	07.13N	100.37E	22.0887
	Phuket	211,000	07.53N	98.24E	2.1819
	Ranong	163,160	9.962N	98.638E	4.27555
	Satun	270,802	6.617N	100.067E	4.61174
20. Taiwan	Hsin-chu	384,384	24.80N	120.98E	12.0184
	Kao-hsiung	1,500,000	22.60N	120.28E	10.563
21. Malaysia	Georgetown	180,573	05.25N	100.20E	4.28901
	Klang(Kelang)	563,173	03.02N	101.26E	6.98943
	Kuala Lumpur	1,297,526	03.09N	101.41E	6.98113
	Melaka	369,222	02.15N	102.15E	8.50881
	Johor Bahru	384,613	01.28N	103.46E	10.8117
	Kuantan	283,041	03.49N	103.20E	16.611
	Kuala Terengganu	250,528	05.20N	103.08E	18.0761
	Kota Bahru	233,673	06.07N	102.14E	20.1728
	Kuching	579,900	01.53N	110.33E	15.4757
	Bintulu	116,600	03.20N	113.02E	12.503
	Kota Kinabalu	24,821,286	05.98N	116.06E	11.1984
	Sandakan	24,385,858	05.86N	118.06E	9.18603
22. Brunei	Bandar Seri	46,229	04.93N	114.96E	11.8372
23. Indonesia	Jayapura	145,200	02.28S	140.38E	9.13068
	Namlea	124,084	03.25S	127.12E	6.28019
	Ambon	313,100	03.43S	128.12E	6.35841
	Bula	57,474	03.12S	130.45E	6.94673
	Tobelo	3,860	01.75N	127.98E	7.77472
	Manado	398,900	01.29N	124.51E	7.55753
	Majene	1,268,500	03.55S	118.98E	5.94927
	Ujung Pandang	1,091,800	05.10S	119.20E	5.7257
	Kupang	165,500	10.22S	123.63E	5.12295
	Sumbawa Besar	52,654	08.50S	117.42E	4.87692
	Mataram	306,600	08.35S	116.07E	4.21647
	Denpasar	435,000	08.39S	115.13E	4.10912
	Surabaya	3,092,400	07.17S	112.45E	8.02103
	Semarang	1,366,500	07.00S	110.26E	7.81216
	Yogyakarta	419,500	07.49S	110.22E	3.41068
	Jakarta	8,987,800	06.09S	106.49E	4.7177

(*Contd.*)

Table 3. (*Contd.*)

Country	*City*	*Population*[#]	*Location*		*Arrival time (hour)*
			Latitude (Degree)	*Longitude (Degree)*	
	Genteng	79,652	07.35S	106.33E	2.6125
	Bandar Lampung	832,400	05.30S	104.30E	2.45704
	Mentok	26,709	02.07S	105.20E	10.3857
	Tanjungbalai	142,506	01.00N	103.32E	11.2742
	Langsa	117,256	04.47N	97.98E	3.17407
	Banda Aceh	291,300	05.35N	95.20E	0.761689
	Meulaboh	4,775	04.17N	96.15E	0.567799
	Sibolga	22,513	01.70N	98.80E	1.97274
	Padang	721,500	01.00S	100.20E	1.80631
	Bengkulu	262,100	03.50S	102.12E	2.24429
	Pontianak	449,100	00.03S	109.15E	12.8599
	Ketapang	1,680	01.83S	109.98E	10.7732
	Bandjarmasin	534,600	03.20S	114.35E	10.1546
	Balikpapan	448,700	01.25S	116.83E	7.54061
	Tarakan	98,800	03.33N	117.63E	7.71036
24. Madagascar	Antsiranana	220,000	12.25S	49.20E	8.3672
	Antalaha	75,000	14.88S	50.27E	7.67597
	Toamasina	230,000	18.10S	49.25E	7.91618
	Manakara	25,689	22.15S	48.00E	8.2238
	Cape St Marie	31,592,805	25.57S	45.17E	9.50308
	Toliary	150,000	21.50S	43.74E	10.3438
	Morondava	33,372	20.32S	44.28E	10.4581
	Tambohorano	406,564	17.50S	43.59E	9.63051
	Mahajanga	200,000	15.40S	46.25E	8.71684
	Hell Ville	23,050	13.40S	48.28E	8.62156
25. Seychelles	Victoria	20,050	04.63S	55.47E	7.37542
26. Comoros	Moroni	629,000	11.67S	43.27E	8.69479
	Dzaoudzi	690,948	12.80S	45.30E	8.42018
27. Maldives	Male	74,069	04.00N	73.00E	4.09193
28. Mauritius	Port Louis	127,855	20.10S	57.30E	6.87434
29. Reunion	Saint-Benoit	101,804	21.03S	55.71E	7.01025
	Saint-Denis	236,599	20.87S	55.46E	7.07017
	Saint-Paul	138,551	21.00S	55.27E	7.3678
	Saint-Pierre	229,346	21.27S	55.53E	7.14395
30. Sri Lanka	Kankesanturai	31,506	9.85N	80.08E	4.09997
	Mullaittivu	7,900	09.25N	80.80E	3.09918
	Trincomalee	91,000	08.38N	81.15E	3.13302
	Batticaloa	515,707	7.72N	77.73E	3.46255
	Okanda	9,594	06.65N	81.77E	2.55246
	Hambantota	11,734	6.12N	81.12E	2.67229
	Matara	643,786	5.95N	80.55E	2.73498
	Galle	97,000	06.05N	80.10E	2.88227
	Moratuwa	177,190	06.45N	79.55E	2.93046

(*Contd.*)

(*Contd.*)

	Dehiwala-Lavinia	209,787	06.51N	79.52E	2.94426
	Colombo	642,163	05.56N	79.58E	2.80593
	Negombo	121,933	07.12N	79.50E	3.08903
	Talalla	78,023	08.13N	79.70E	3.38355
	Mannar	106,235	8.98N	79.92E	4.41793
	Jaffna	177,190	09.45N	80.02E	4.71506
31. Singapore	SingaporeCity	4,163,700	01.22N	103.55E	10.948
32. Philippines	Laoag	89,468,677	18.23N	120.60E	10.2071
	Quezon City	2,173,831	14.38N	121.00E	11.1002
	Manila	1,581,082	14.40N	121.03E	11.1002
	Bulan	28,529	12.66N	123.88E	9.406
	Mindaro	81,159,644	13.00N	121.00E	9.89557
	Iloilo	365,820	10.68N	122.55E	9.27341
	Cebu City	718,821	10.18N	123.54E	9.73164
	Siaton	64,258	09.08N	123.08E	8.67981
	Palawan Is	737,000	9.50N	118.50E	8.81906
	Zamboanga City	601,794	06.54N	122.04E	7.76695
	Davao	1,725,355	7.08N	125.63E	8.23129
33. Australia	Melbourne	3,488,800	37.50S	145.00E	12.5851
	Adelaide	1,110,500	34.52S	138.30E	12.121
	Nhulunbuy	3,202	12.50S	136.93E	14.293
	Crocker	14,375	11.03S	136.63E	11.7589
	Bathurst I	37,001	11.75S	130.68E	9.78129
	Darwin	108,200	12.25S	130.51E	9.47687
	C. St Lambert	20,976	14.28S	127.71E	9.12529
	C. Leveque	12,330	16.41S	122.91E	6.05995
	Broome	13,218	17.97S	122.25E	6.53677
	Port Hedland	14,288	20.40S	118.60E	7.00693
	Dampier Downs	770	18.52S	123.45E	9.1031
	Onslow	700	21.68S	115.20E	5.95066
	Exmouth	2,400	21.90S	114.16E	5.10908
	Carnarvon	7,392	24.85S	113.75E	6.38753
	Kalgoorlie	36,852	27.70S	114.16E	6.50292
	Geraldton	27,258	28.81S	114.60E	6.23176
	Perth	1,397,000	31.57S	115.52E	6.28896
	Bunbury	26,369	33.33S	115.56E	6.77029
	Albany	23,913	34.95S	117.90E	7.10817
34. Vietnam	Haiphong	1,447,523	20.47N	106.41E	15.1392
	Hon Gai	129,394	20.57N	107.05E	14.7076
	Vinh	175,167	18.45N	105.38E	14.4124
	Dong Hoi	40,290	17.53N	106.58E	13.7196
	Hue	260,489	16.30N	107.35E	13.3015
	Da Nang	369,734	16.04N	108.13E	12.9678
	Qui Nhon	201,972	13.40N	109.13E	12.1071
	Nha Trang	263,093	12.16N	109.10E	12.1088
35. India	Rapur	5,380	23.05N	68.83E	8.71781
	Kandla	175,000	23.00N	70.10E	10.1083
	Dwarka	33,614	22.25N	69.05E	7.96334

(*Contd.*)

Table 3. (*Contd.*)

Country	*City*	*Population*[#]	*Location*		*Arrival time (hour)*
			Latitude (Degree)	*Longitude (Degree)*	
	Porbandar	133,083	21.44N	69.43E	6.99742
	Veraval	141,207	20.53N	70.27E	7.22848
	Diu	21,576	20.40N	71.02E	7.74814
	Bhavnagar	510,958	21.45N	72.10E	9.10254
	Daman	113,949	20.25N	72.57E	8.5291
	Dadar & Nagar Haveli	220,451	20.05N	73.00E	8.63183
	Mahim	42,798	19.66N	72.76E	8.55693
	Mumbai	11,914,398	18.55N	72.50E	7.47182
	Ratnagiri	70,335	17.13N	73.32E	7.14562
	Malvan	18,675	16.05N	73.50E	6.58475
	Panaji	1,170,000	15.25N	73.50E	5.92902
	Murmagao	189,383	15.25N	73.56E	5.99745
	Karwar	62,960	14.83N	74.15E	6.28768
	Kumta	27,597	14.48N	74.41E	6.26771
	Bhatkal	31,785	13.96N	74.58E	6.04996
	Mangalore	398,745	12.55N	74.47E	5.01031
	Kozhikode	2,613,683	11.15N	75.43E	4.7295
	Cochin(Kochi)	550,000	09.58N	76.20E	4.64342
	Quilon(Kollam)	391,300	08.90N	76.63E	4.64503
	Trivandrum	744,739	08.41N	77.00E	4.17903
	Kanyakumari	208,149	08.07N	77.58E	3.92992
	Thoothukkudi	216,058	08.50N	78.12E	3.73327
	Rameswaram	38,035	09.28N	79.37E	3.90142
	Nagapattinam	94,965	10.77N	79.88E	3.56652
	Karaikal	170,640	10.59N	79.50E	4.57374
	Pondicherry	735,004	11.59N	79.50E	3.36741
	Chennai	4,216,268	13.08N	80.19E	3.57933
	Nellore	378,947	14.27N	79.59E	3.71164
	Chirala	85,455	15.98N	80.08E	4.22424
	Machilipatnam	215,043	16.15N	81.20E	4.08971
	Visakhapatnam	969,608	17.45N	83.20E	3.64451
	Gopalpur	114,189	19.27N	84.95E	4.21065
	Puri	157,610	19.50N	85.58E	3.79441
	Haldia	170,695	22.03N	88.03E	5.62307
	Henhoaha	1,018	06.80N	93.81E	0.961126
	Misha	2,660	08.00N	93.36E	1.44183
	Kakana	4,291	09.11N	92.81E	1.58246
	Nachuge	2,233	10.71N	92.35E	2.06832
	Port Blair	100,186	11.68N	92.77E	1.92749
	Coco Channel	2,233	14.08N	93.30E	2.46952
	Kavaratti Is	10,113	10.53N	72.71E	4.52211
	Androth Is	10,000	11.00N	73.16E	4.54489
	Chetlat Is	51,707	11.76N	76.83E	5.38175
	Minicoy Is	9,957	08.48N	73.02E	4.20262

[#] *Population database is based on the latest information available through various sources from internet.*

7.2 Network Learning Principles and Algorithms

The input is transformed to an output through the hidden layers. Input vectors and the corresponding output (target) vectors are used to train the network until it can approximate a function, associate input vectors with specific output vectors, or classify input vectors in an appropriate way as defined. It has been shown that networks with biases, sigmoid layers and a linear output layer are capable of approximating any function with a finite number of discontinuities. In the present work, the back-propagation feed forward type network is used for training the system where the objective is to minimize the global error E given as:

$$E = \frac{1}{P}\sum E_p \tag{4}$$

and

$$E_P = \frac{1}{2}\sum (o_k - t_k^2) \tag{5}$$

where P is the total number of training patterns (the number of input/output pairs used for training), E_p is the error for the p-th pattern, o_k is the network output at the k-th output node and t_k is the target output at the k-th output pattern.

In this type of network the error between the target output and the network output are calculated and this is back propagated. The term back-propagation refers to the manner in which the gradient is computed for nonlinear multilayer networks. Standard back-propagation is a gradient descent algorithm. There are a number of variations on the basic algorithm that are based on other standard optimization techniques. A brief description on the working principle of a back-propagation neural network is given below.

7.3 Back-Propagation Learning

Back-propagation is a widely used algorithm for supervised learning with a multilayer feed forward layer network which implements the repeated application of the chain rule to compute the influence of each weight in the network with respect to an arbitrary error function E (Dayhoff, 1990):

$$\frac{\partial E}{\partial w_{ij}} = \frac{\partial E}{\partial s_i}\frac{\partial s_i}{\partial net_i}\frac{\partial net_i}{\partial w_{ij}} \tag{6}$$

In the above equation [Eqn. (6)], w_{ij} is the weight from the neuron j to neuron i, s_i is the output, and net_i is the weighted sum of the inputs of neuron i. Once the partial derivative for each weight is known, the error function is minimized by performing a simple gradient descent (Zurada, 1992):

$$w_{ij}(t+1) = w_{ij}(t) - \varepsilon \frac{\partial E(t)}{\partial w_{ij}} \tag{7}$$

7.4 Resilient Back-Propagation Learning

Multilayer networks typically use sigmoid transfer functions in the hidden layers. Sigmoid functions cause a problem while training a multilayer network using steepest descent since they compress an infinite input range into a finite output range and are characterized by the fact that their slope must approach zero as the input gets large. The gradient can have a very small magnitude; and therefore, cause small changes in the weights and biases, even though the weights and biases are far from their optimal

values. The purpose of the resilient back-propagation training algorithm is to eliminate contamination in the magnitudes of the partial derivatives. Only the sign of the derivative is used to determine the direction of the weight update; the magnitude of the derivative has no effect on the weight update. This adaptive update value evolves during the learning process based on its local sight on the error function E, according to the following learning rule (Reidmiller and Braun, 1993):

$$\Delta_{ij}^{(t)} = \begin{cases} \eta^{+}\Delta_{ij}^{(t-1)}, & \text{if } \dfrac{\delta E^{(t-1)}}{\delta w_{ij}} \dfrac{\delta E^{(t-1)}}{\delta w_{ij}} > 0 \\ \eta^{-}\Delta_{ij}^{(t-1)}, & \text{if } \dfrac{\delta E^{(t-1)}}{\delta w_{ij}} \dfrac{\delta E^{(t-1)}}{\delta w_{ij}} < 0 \\ \Delta_{ij}^{(t-1)}, & \text{else} \end{cases} \quad \text{where } 0 < \eta^{-} < 1 < \eta^{+} \tag{8}$$

$$\Delta w_{ij}^{(t)} = \begin{cases} -\Delta_{ij}^{(t)}, & \text{if } \dfrac{\delta E^{(t)}}{\delta w_{ij}} > 0 \\ +\Delta_{ij}^{(t)}, & \text{if } \dfrac{\delta E^{(t)}}{\delta w_{ij}} < 0 \\ 0, & \text{else} \end{cases} \tag{9}$$

$$w_{ij}^{(t+1)} = w_{ij}^{(t+1)} + \Delta w_{ij}^{(t)} \tag{10}$$

The resilient back-propagation algorithm has been used in this study to train the neural network system.

8. NETWORK ARCHITECTURE AND PARAMETERS

The performance of the network depends on the network architecture and network parameters chosen to model the system. Extensive trial and error tests have been performed with the comprehensive ETA database (Barman et al., 2006). Based on this study, configurations mentioned below are near optimum for the current prediction model.

8.1 Network Architecture

The optimum parameters of network architecture for prediction of tsunami travel time were chosen with the configuration comprising two hidden layers with number of neurons ranging from 25 to 30 in each hidden layer (recommended value for this study is 30). The transfer functions comprise the tan-sigmoid functions in the hidden layers and the linear transfer function in the output layer. This is a useful structure for regression problems.

8.2 Network Parameters

Based on an earlier study (Barman et al., 2006), the following parameters are recommended as an optimum configuration of the ANN network:

(i) Mean Squared Error (MSE) used in this study is 0.25.
(ii) Learning Rate and Momentum Factor: It was found that the performance of resilient back-propagation is not very sensitive to the settings of these training parameters.

The resilient back-propagation has been used to train the system as we noticed convergence to the specified MSE is obtained very fast using this algorithm. In fact, not many algorithms are able to converge to the specified error level. Besides Resilient back-propagation, we used another algorithm called Levenberg-Marquardt (More, 1978) which is also able to converge, but it was found that the time of convergence is much greater than the former, typically about 100 times or so.

Prudently trained back-propagation network performs significantly well and tends to deliver reasonable estimates when presented with input parameters. Typically, a new input leads to an output similar to the correct output for input vectors used in training that are similar to the new input being presented. This generalization property makes it possible to train a network on a representative set of input/target pairs and get good results without training the network on all possible input/output pairs.

8.3 Training and Testing of ANN Model

For this study, 240 data points of past earthquake locations in the Indian Ocean taken from the ETA database were used. For each of this earthquake event, we have computed tsunami travel time to 250 coastal destinations in the 35 countries surrounding the Indian Ocean rim which is published in the TTT atlas for Indian Ocean. Using the above defined network parameters, we demonstrated that ANN model is quite robust in tackling the non-linearity in the ETA database (Barman et al., 2006). Numerical experiments were conducted with different combinations of data-points within the ETA database. In this experiment, grouping of data within ETA is under two steps: (i) first set for training and testing, and (ii) second set for validation which is not exposed to ANN during the learning stage. This set is used to check the performance of the network with unseen data, and thus gives a measure of the network skill with real-time data. Since performance of ANN solely depends on the nature of data being trained, the performance of ANN model is questionable for a new earthquake location which is not within close vicinity of TTT model. Hence, a situation which is rare to the training and testing set cannot be predicted well. For the Indian Ocean, as seen in Fig. 2, considering the homogeneity in the distribution of earthquake locations from past tsunami-genic events the highest degree of probability for an earthquake is within the vicinity of Sumatra, Indonesia, etc. Therefore, under this circumstance the nonlinear technique based on ANN can be suitably used for a real-time prediction of ETA for countries surrounding the Indian Ocean rim.

9. SIMULATION RESULTS

The results of ETA simulations using ANN with different network configurations for coastal destinations in India (47 locations) are presented below. To study the effectiveness of the nonlinear technique, the selection of validation points from ETA database was judicially grouped into three categories. Of the total 240 locations, skill assessments were performed with 80, 60 and 48 points, respectively as shown in Tables 4, 5 and 6. High values of correlation (around 95%) between the model outputs and the observations

shown in Tables 4, 5 and 6 suggest the feasibility of the model that can predict tsunami arrival time when the underwater earthquake locations is provided within the study domain.

The correlation between the known and predicted ETA using three different combinations of data for an optimally trained network with two hidden layers using 30 neurons each trained to a mean square error of 0.25 using the resilient back-propagation is shown in Figs 5, 6 and 7 corresponding to Tables 4, 5 and 6, respectively. An optimum selection of 25 neurons each was found to be sufficient keeping in mind the skill factor of prediction of ETA using ANN.

Table 4. Simulation results for 80 validation data when trained with 160 data (Combination 1)

Validation Data: 1 out of every 3 in ETA Database

Total number of data	240	Number of inputs	2
Training-Testing data	160	Number of outputs	47
Validation data	80		

Neurons	*Goal*	*Training time (minutes)*	*Training correlation*	*Validation correlation*		
				Minimum	*Maximum*	*Average*
[20 20]	0.3	1	0.9799	0.945	0.9603	0.9553
[20 20]	0.25	1	0.9833	0.929	0.9632	0.9525
[20 20]	0.2	2	0.9866	0.9465	0.9658	0.9563
[25 25]	0.3	1	0.9802	0.9406	0.9692	0.9537
[25 25]	0.25	1	0.9834	0.9289	0.9539	0.9429
[25 25]	0.2	1	0.9866	0.9103	0.9475	0.9252
[30 30]	0.3	1	0.9801	0.9322	0.966	0.955
[30 30]	0.25	1	0.9834	0.9436	0.968	0.959
[30 30]	0.2	1	0.9866	0.9486	0.9655	0.9585

Table 5. Simulation results for 60 validation data when trained with 180 data (Combination 2)

Validation Data: 1 out of every 4 in ETA Database

Total number of data	240	Number of inputs	2
Training-Testing data	180	Number of outputs	47
Validation data	60		

Neurons	*Goal*	*Training time (minutes)*	*Training correlation*	*Validation correlation*		
				Minimum	*Maximum*	*Average*
[20 20]	0.3	1	0.979	0.9866	0.9886	0.9874
[20 20]	0.25	2	0.9819	0.9711	0.9797	0.9755
[20 20]	0.2	3	0.9855	0.979	0.9844	0.9809
[25 25]	0.3	1	0.9782	0.961	0.9772	0.9686
[25 25]	0.25	1	0.9819	0.9601	0.9718	0.967
[25 25]	0.2	8	0.9855	0.8206	0.8592	0.8431
[30 30]	0.3	1	0.9783	0.9544	0.9688	0.9615
[30 30]	0.25	1	0.9819	0.9652	0.9754	0.9667
[30 30]	0.2	> 10	0.9842	0.9585	0.9699	0.9651

Table 6. Simulation results for 48 validation data when trained with 192 data (Combination 3)

Validation Data: 1 out of every 5 in ETA Database			
Total number of data	240	Number of inputs	2
Training-Testing data	192	Number of outputs	47
Validation data	48		

Neurons	*Goal*	*Training time (minutes)*	*Training correlation*	*Validation correlation*		
				Minimum	*Maximum*	*Average*
[20 20]	0.3	1	0.9784	0.943	0.9518	0.9471
[20 20]	0.25	1	0.9821	0.941	0.9567	0.9513
[20 20]	0.2	1	0.9856	0.951	0.9597	0.9573
[25 25]	0.3	1	0.9785	0.9452	0.9624	0.9545
[25 25]	0.25	1	0.9821	0.9503	0.9572	0.9534
[25 25]	0.2	1	0.9857	0.9464	0.9557	0.9511
[30 30]	0.3	1	0.9786	0.9489	0.9612	0.9543
[30 30]	0.25	1	0.984	0.9497	0.9588	0.9548
[30 30]	0.2	1	0.9856	0.9402	0.9554	0.9485

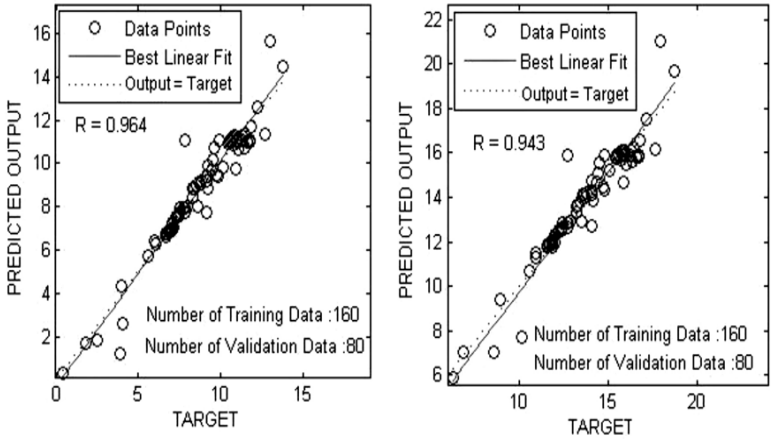

Fig. 5 Actual and predicted outputs (Validation data, Combination 1) for the best correlated output (Left) and the worst correlated output (Right) for 47 coastal locations in Indian sub-continent.

10. CONCLUDING REMARKS

An effective tsunami early warning system is achieved when all persons in vulnerable coastal communities are prepared and respond appropriately, and in a timely manner, upon recognition that a potentially destructive tsunami is approaching. Timely tsunami warnings issued by a recognized tsunami warning center are essential. When these warning messages are received by the designated government agency, tsunami emergency response plans must already be in place so that well-known and practiced actions are

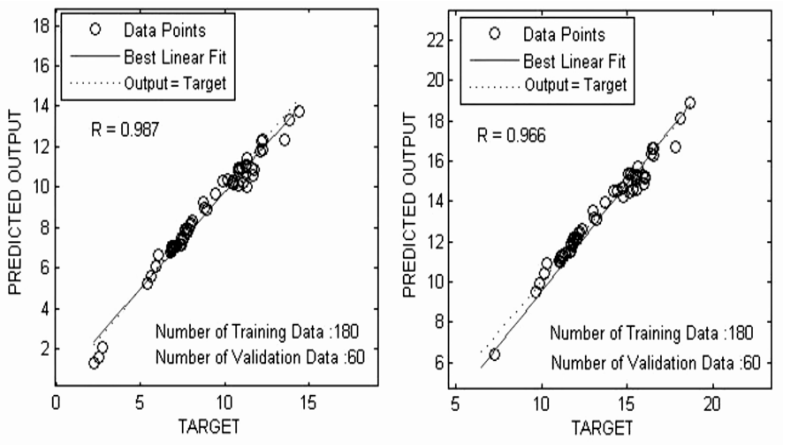

Fig. 6 Actual and predicted outputs (Validation data, Combination 2) for the best correlated output (Left) and the worst correlated output (Right) for 47 coastal locations in Indian sub-continent.

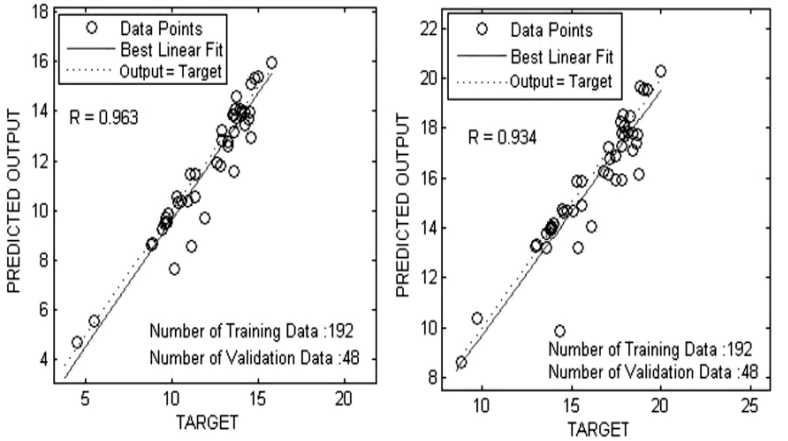

Fig. 7 Actual and predicted outputs (Validation data, Combination 3) for the best correlated output (Left) and the worst correlated output (Right) for 47 coastal locations in Indian sub-continent.

immediately taken to evaluate the scientifically-based warning, and communicate an appropriate course of action to ordinary citizens. Tsunami preparedness programs must be implemented on a national level so that good decisions can be made without delay.

In this chapter, we discussed travel times for the first wave of tsunami approaching the coast which has been subsequently verified by the computation carried out for the recent December 2004 Indian Ocean tsunami from tide gauges as well as signatures of satellite tracks. It does not provide information

on the arrival times of subsequent waves, nor does it provide information on how many waves will be in the tsunami event, which wave in succession will be the highest, at what time each wave will arrive at a given location on the coast line, the run-up along littoral belts and resulting inundation, how strong the currents will be in each wave, exactly at what locations should people and domestic animals be evacuated, how long should they be evacuated, at what time it will be safe for them to return, nonlinear dispersive effects of tsunami waves, etc. To obtain detailed information about all these parameters, separate numerical models of tsunami generation and propagation, and of coastal inundation should be developed. The importance of such study in computing TTT is to extend this computational algorithm for multiple tsunami-genic locations in the Indian Ocean rim facilitating development of ETA database. This basic information can be used as extremely important database for early response in the development of tsunami warning systems.

We demonstrated here how soft computing tools like ANN could handle the non-linear system where the prediction of ETA at different coastal destinations of Indian sub-continent is achieved in a real-time mode. The algorithm uses earthquake locations and computed travel time from the ETA database. It could be advocated that the major advantage of using ANN in a real-time tsunami travel time prediction is its high merit in producing ETA at a much faster time and simultaneously preserving the consistency of prediction. The model using ANN performs a rapid computation of ETA (on average of four seconds) compared to the conventional travel time model which takes approximately 60 minutes. The correlation is found very high for the unseen data as noted from different combinations of training and testing the ANN. The importance of this model is highly justified for a tsunami warning system where the time involved in computing ETA and the issue of warning messages to coastal destination is a critical factor. The proposed method is expected to have direct practical applications for a real-time tsunami warning system for the Indian Ocean as well as the global oceans. For the benefit of the readers, an atlas on comprehensive database of Tsunami Travel Time for the Indian Ocean is available at http://www.iitkgp.ac.in/topfiles/tsunami.html. Finally, the validation capability of the model was found to be satisfactory and reliable which suggests its applicability for real-time prediction.

In context of known natural disasters such as earthquakes, floods, cyclones, storm surges, landslides, volcanic eruptions, etc., warning systems exist for most of these disasters except for earthquakes. Developed nations like the USA and Japan are prepared to cope even with earthquakes. Hence, developing nations need to gear up with technology which can be helpful in the event of natural disasters. In case of a tsunami event, the basic and vital information is the time of arrival at various coastal destinations of a nation and hinterland. In this context, we demonstrated the importance of ANN as a tool for an effective tsunami warning system. However, an effective tsunami warning system is a composite feedback mechanism starting from *in situ* bottom pressure sensors, communication linkage from sensors via satellite to land-based stations and final processing of information at a nodal agency for an alert warning to various coastal destinations. The discussion in this chapter pertains to the computation of TTT and how this vital information can be expedited using soft computing tools like ANN. For the operational purpose, database within ETA needs to be periodically updated by TTT computations for earthquake locations which is the future scope not covered in this study. Overall, it can be concluded that modern technology can prevent or help in minimizing the loss of life and property provided we integrate all essential components in the warning system and put it to the best possible use.

REFERENCES

Bapat, A., Kulkarni, R.C. and Guha, S.K. (1983). Catalog of Earthquakes in India and Neighborhood from Historical Period up to 1979. Ind. Soc. Earthq. Tech., Roorkee, 211 pp.

Barman, R., Prasad, K.B., Pandey, P.C. and Dube, S.K. (2006). Tsunami travel time prediction using neural networks. *Geophysical Research Letters,* **33:** L16612, doi:10.1029/2006GL026688.

Bindra, S. (2005). Tsunami: 7 Hours that Shook the World. Harper Collins Publications, New Delhi, India, 291 pp.

Bishop, C.M. (1995). Neural Networks for Pattern Recognition. Oxford University Press, Oxford, U.K., pp. 364-369.

Chapman, C. (2005). The Asian tsunami in Sri Lanka: A personal experience. EOS, *Transactions American Geophysical Union*, **86(1):** 13-14.

Dayhoff, J.E. (1990). Neural Network Architecture: An Introduction. Van Nostrand Reinhold, New York, 259 pp.

Hanson, J.A. and Bowman, J.R. (2005). Dispersive and reflected tsunami signals from the 2004 Indian Ocean tsunami observed on hydrophones and seismic stations. *Geophysical Research Letters*, **32:** L17606, doi:10.1029/2005GL023783.

Hinton, G.E. (1992). How neural networks learn from experience. *Sci. Amer*., **9:** 144-151.

Holloway, G., Murty, T.S. and Fok, E. (1986). Effects of bathymetric roughness upon tsunami travel time. *Science of Tsunami Hazards*, **4(3):** 165-172.

Li, S., Hsieh, W.W. and Wu, A. (2005). Hybrid coupled modeling of the tropical Pacific using neural networks. *J. Geophys. Res*., **110:** C09024, doi:10.1029/2004JC002595.

Lietzin, E. (1974). Sea Level Changes. Elsevier Oceanographic Series, No. 8, New York, 273 pp.

More, J.J. (1978). The Levenberg-Marquardt Algorithm: Implementation and Theory. *In:* G.A.Watson (editor), Lecture Notes in Mathematics, 630, Springer-Verlag, Berlin, pp. 105-116.

Murty, T.S. (1984). Storm Surges – Meteorological Ocean Tides. *Canadian Bulletin of Fisheries and Aquatic Sciences*, **212**, Department of Fisheries and Oceans, Ottawa, Canada, 897 pp.

Murty, T.S., Saxena, N.K., Sloss, P.W. and Lockridge, P.A. (1987). Accuracy of tsunami travel time charts. *Marine Geodesy*, **11:** 89-102.

Navone, H.D. and Ceccatto, H.A. (1994) Predicting Indian monsoon rainfall: A neural network approach. *Climate Dynamics*, **10**(6): 305-312.

Okal, E.A., Plafker, G., Synolakis, C.E. and Borrero, J.C. (2002). Near-field survey of the 1946 Aleutian tsunami on Unimak and Sanak Islands. *Bulletin Seismological Society of America*, **93:** 1226-1234.

Orman, J.V., Cochran, J.R., Weissel, J.K. and Jestin, F. (1995). Distribution of shortening between the Indian and Australian plates in the central Indian Ocean. *Earth and Planetary Science Letters*, **133(1-2):** 35-46.

Pendse, C.G. (1945). The Mekran Earthquake of the 28th November 1945. *India Meteor. Department Scientific Notes*, **10(25):** 142-145.

Prasad, K.B., Dube, S.K., Murty, T.S., Gangopadhyay, A., Chaudhuri, A. and Rao, A.D. (2005). Tsunami Travel Time Atlas for the Indian Ocean. CORAL, Indian Institute of Technology Kharagpur, West Bengal, India, 286 pp.

Prasad, K.B., Rajesh, K.R., Dube, S.K., Murty, T.S., Gangopadhyay, A., Chaudhuri, A. and Rao, A.D. (2006). Tsunami travel time computation and skill assessment for the 26 December 2004 event in the Indian Ocean. *Coastal Engineering Journal*, **48(2):** 147-166.

Reidmiller, M. and Braun, H. (1993). A direct adaptive method for faster back-propagation learning: The RPROP algorithm. Proc. IEEE Int. Conf. on Neural Networks, San Francisco, pp. 586-591.

Silverman, D. and Dracup, J. (2000). Artificial neural networks and long range precipitation prediction in California. Journal *of Applied Meteorology*, **31(1)**: 57-66.

Simon, H. (1998). Neural Networks: A Comprehensive Foundation. 2nd Edition, Prentice-Hall, Englewood Cliffs, New Jersey, 842 pp.

Synolakis, C.E. (1995). Tsunami prediction. *Science*, **270:** 15-16.

Tandon, A.N. and Srivastava, H.N. (1974). Earthquake Occurrence in India: Earthquake Engineering. Sarita Prakashan, Meerut, 48 pp.

Venkatesan, C., Raskar, S.D., Tambe, S.S., Kulkarni, B.D. and Keshavamurty, R.N. (1997). Prediction of all India summer monsoon rainfall using error-back-propagation neural networks. *Meteorology and Atmospheric Physics*, **62**: 225-240.

Yeh, H., Liu, P., Briggs, M. and Synolakis, C.E. (1994). Tsunami catastrophe in Babi Island. *Nature*, **372:** 6503-6508.

Yong, W., Kwok, F.C., George, D.C. and Charles, S.M. (2003). Inverse algorithm for tsunami forecasts. *Journal of Waterway, Port, Coastal and Ocean Engineering*, **129(2):** 60-69.

Yuri, I.S. and Leonid, B.C. (1995). Mathematical modeling in mitigating the hazardous effect of tsunami waves in the ocean: A priori analysis and timely on-line forecast. *Science of Tsunami Hazards*, **13(1):** 27-44.

Zetler, B.D. (1947). Travel time of seismic sea waves to Honolulu. *Pacific Science*, **1(203):** 185-188.

Zurada, J.M. (1992). Introduction to Artificial Neural Systems. West Publishing Company, St. Paul, Minnesota, 785 pp.